

This paper is a post-print version of a final paper published in:

Šarić, Ana, et al. "Non-Toxic Fluorescent Phosphonium Probes to Detect Mitochondrial Potential." *Methods and Applications in Fluorescence*, vol. 5, no. 1, Mar. 2017, p. 015007. *DOI.org (Crossref)*, doi:10.1088/2050-6120/aa5e64.

PAPER

Non-toxic fluorescent phosphonium probes to detect mitochondrial potential

Ana Šarić^{1,2}, Ivo Crnolatac³, Frédéric Bouillaud⁴, Sandra Sobočanec^{1,6}, Ana-Matea Mikecin¹, Željka Mažak Šafranko¹, Todor Delgeorgiev⁵, Ivo Piantanida³, Tihomir Balog¹ and Patrice X Petit²

¹ Division of Molecular Medicine, Ruđer Bošković Institute, Zagreb, Croatia

² INSERM U1124 University Paris Descartes, Paris, France

³ Division of Organic Chemistry and Biochemistry, Ruđer Bošković Institute, Zagreb, Croatia

⁴ Department of Endocrinology, Metabolism and Cancer—INSERM U567, CNRS UMR 8104, Institut Cochin—University Paris Descartes, Paris, France

⁵ Faculty of Chemistry and Pharmacy, University of Sofia, Sofia, Bulgaria

⁶ Equal contribution to this work.

E-mail: ssoboc@irb.hr

Keywords: mitochondria, membrane potential, flow cytometry, confocal microscopy, toxicity analysis, respiration, probe Supplementary material for this article is available [online](#)

Abstract

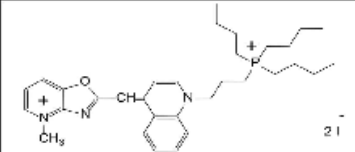
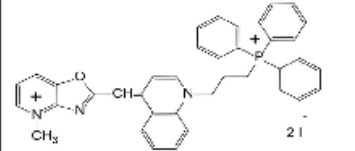
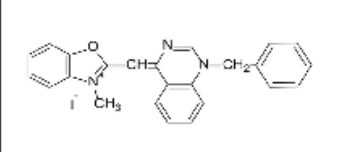
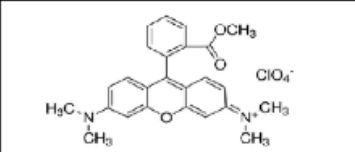
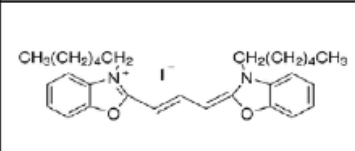
We evaluated our phosphonium-based fluorescent probes for selective staining of mitochondria. Currently used probes for monitoring mitochondrial membrane potential show varying degrees of interference with cell metabolism, photo-induced damage and probe binding. Here presented probes are characterised by highly efficient cellular uptake and specific accumulation in mitochondria. Fluorescent detection of the probes was accomplished using flow cytometry and confocal microscopy imaging of yeast and mammalian cells. Toxicity analysis (impedimetry—xCELLigence for the cellular proliferation and Seahorse technology for respiratory properties) confirms that these dyes exhibit no-toxicity on mitochondrial or cellular functioning even for long time incubation. The excellent chemical and photophysical stability of the dyes makes them promising leads toward improved fluorescent probes. Therefore, the probes described here offer to circumvent the problems associated with existing-probe's limitations.

Introduction

Mitochondria are cellular 'power plants' which control cellular life and death. There is a growing list of diseases and pathological processes in which mitochondrial dysfunction is implicated [1]. An electrochemical proton gradient exists across the mitochondrial inner membrane as a result of proton pumping by respiratory chain components located within this membrane. The resulting gradient of mitochondrial membrane potential ($\Delta\Psi_m$) is the major force that drives aerobic energy production by generating adenosine triphosphate (ATP)—a universal energy currency of the cell. Mitochondrial loss of $\Delta\Psi_m$ plays a pivotal role in cell death [2] and $\Delta\Psi_m$ provides one of the most valuable indicators of cells' functional status. Therefore, the accurate measurement of $\Delta\Psi_m$ is essential to deduce the role of mitochondria in apoptotic process, disease and ageing [3].

Fluorescent probe technology exploits the partition principle of fluorescent lipophilic cations or 'redistribution dyes' between cellular compartments in proportion to the standing electrochemical gradients. Phosphonium conjugates are often used as ligands to serve in a mitochondriotropic purpose, in a whole range of different applications including measuring hydrogen peroxide levels [4], monitoring oxygen variation within mitochondria or as carriers to specifically target nanoparticles in theranostic medicine in photodynamic therapy [5, 6]. The uptake of most mitochondria-selective dyes is dependent of $\Delta\Psi$, with a few exceptions including exception nonyl acridine orange (NAO) and Mito-Tracker Green FM capable of staining mitochondria regardless of their polarization status [7]. The fluorescence of cells stained with this type of dye is directly proportional to their content of mitochondria (i.e., the mitochondrial mass). This is allowed by the affinity of these dyes with mitochondrial-specific components.

Table 1. Structure and characteristics of the dyes used in this work.

Probe	Structure	Excitation maximum (nm)	Emission maximum (nm)
TD2-1		518	547
TD2-2		519	547
TD4-5		440	489
TMRM		550	580
DiOC ₆ (3)		482	504

Fluorescent dye accumulation in mitochondria is then detected by microscopy, flow cytometry or fluorescence plate reader, allowing comparative assessments of $\Delta\Psi_m$ among experimental conditions (e.g. health versus disease) [8]. The existing probe technologies may often be misleading and may account for some of the discrepancies in this research area, since currently available probes are subject to artefacts. For example, JC-1 probe can only detect large differences in membrane potential across regions or populations of cells [8, 9]. DiOC₆(3) (3,3'-dihexyloxacarbocyanine iodide) is known to be a potent inhibitor of respiration and endoplasmic reticulum binder as well [10]. Rhodamine 123 has been shown to inhibit the mitochondrial F₀F₁-ATPase when used in the micromolar range at external concentration [11]. The least toxic to mitochondria of all commonly used probes, TMRM (tetramethylrhodamine methyl ester), can be used in concentrations only up to 0.5 μ M without causing an inhibitory effect on respiration [12]. Thus, despite the apparent abundance of mitochondria-targeted fluorescence probes, development of improved artefact-free indicator probes represents a prerequisite for the valid mitochondrial function assessment.

In previous work, we prepared novel asymmetric phosphonium cyanine dyes based on benzothiazole-quinoline conjugates with new types of sterically demanding,

yet positively charged phosphonium substituents [13, 14]. We showed that by modifying the substituents on the dyes we can manipulate their cellular toxicity. Simultaneously, phosphonium substituents were used to specifically target mitochondria [15]. As a result, the presented dyes combine very low cytotoxicity (as determined by classic MTT test) with efficient cellular uptake as well as fluorescent marking of mitochondria.

In this study, we chosen TD2-1, TD2-2 and TD4-5 (table 1) among the newly developed compounds to be carefully evaluated as novel, improved mitochondria-targeted fluorescent probes to measure the magnitude of $\Delta\Psi_m$ for fluorescence imaging and flow cytometry analysis of mitochondrial function. The work described here offers to circumvent some of the problems associated with existing probe limitations. The potential use of these probes will be interesting to the scientist involved in the research of tumor biology, ageing and ageing related disease, as well as scientist involved in fundamental research of biology and related fields.

Experimental

Materials

Studied dyes were prepared according to previously reported procedures [12, 13]. All chemicals were

purchased from Sigma (St Louis, MO, USA), unless otherwise stated. Concentrated stock solutions (10 mM) of fluorochromes DiOC₆(3), JC-1, TMRM, MitoTracker Deep Red (Invitrogen, Molecular Probes) and TD4-5 were stored at -20 °C. Working solutions were freshly prepared by diluting the stock solutions and kept on ice in the dark to minimise degradation. TD2-1 and TD2-2 were diluted in water (10 mM) and stored at +4 °C.

HeLa and U87-MG cells were obtained from ATCC (American Type Culture Collection, USA) and cultured in DMEM Glutamax I supplemented with 10% fetal calf serum, 1 mM Hepes, 1 mM Napryuvate (Invitrogen).

Wild type *Saccharomyces cerevisiae* Y258 (Thermo-Scientific) and 'petite' yeast strain were kind gift from Anita Kriško (Mediterranean Institute for Life Sciences, Split, Croatia). Yeast strains were grown at 30 °C with shaking on YPD medium containing 2% (w/v) glucose. All experiments were performed on yeast cells from mid-exponential phase: cells were grown until OD 0.6–0.8, harvested by 5 min cen-trifugation at 4000 × g, washed and resuspended to reach a concentration of 10⁶ cells ml⁻¹ adequate for flow cytometry and confocal studies. For staining, the cells were incubated in 1 ml medium supplemented with dyes or no dyes for indicated time periods, protected from light and using thermocycler at 30 °C and 450 rpm.

The experiments with mice were performed in accordance with the current laws of the Republic of Croatia and with the guidelines of European Community Council Directive of 24 November 1986 (86/609/EEC). Efforts were made to minimise stress and discomfort during handling and sacrifice of the animals. Adult female CBA/H mice (20–25 g) 3–4 months old from breeding colony of the Ruđer Bošković Institute (Zagreb, Croatia) were used for mitochondria isolation. The animals were maintained under the following laboratory conditions: light on from 06:00 to 18:00; 22 ± 2 °C room temperature, access to food pellets and tap water ad libitum.

Mitochondria isolation

CBA mice liver mitochondria were isolated by differential centrifugation as described previously [16], with some modifications. Liver was homogenised by ice-packed Potter-Elvehjem homogeniser (Braun, Bio-tech. Int., Germany) at a ratio of 1 g tissue/5 ml of isolation buffer (250 mM sucrose, 2 mM EGTA, 0.5% fatty acid free BSA, 20 mM Tris-HCl, pH 7.4). The homogenate was centrifuged (2000 × g/4 °C/3 min) to discard nuclei and cell debris. The supernatant was spun down (8000 × g/4 °C/10 min) to precipitate mitochondria which were then washed in isolation buffer and centrifuged again (12 000 × g/4 °C/ 10 min) rendering crude mitochondrial fraction. Mitochondria pellet was resuspended in respiration

buffer (RB; 200 mM sucrose, 50 mM KCl, 1 mM MgCl₂ × 6H₂O, 5 mM KH₂PO₄, 20 mM Tris/HCl, pH 7.0) and stored on ice for mitochondrial respiration measurement. Protein concentration was determined by Bradford assay (BioRad Laboratories, Inc.) with BSA as a standard.

Mitochondrial oxygen consumption

Mitochondria (1 mg protein) were incubated in 450 μl respiration buffer supplemented with indicated concentrations of the probes and substrates for 5 min in the dark with constant magnetic stirring at 30 °C. Incubations were done using either 5 mM glutamate and 2.5 mM malate or 5 mM succinate and 2 μM rotenone for complex I or complex II activity assessment, respectively.

After the incubation of mitochondria with or without the dyes, mitochondrial suspension was reoxygenated by vortex and immediately analysed for oxygen consumption. Oxygen uptake was determined polarographically by Clark type electrode (Oxygraph, Hansatech, Norfolk, UK) in an airtight 1.5 ml chamber at 35 °C. After measurement of basal state 4 respiration in the presence of indicated substrates, mitochondrial respiration was accelerated by the addition of 0.5 mM ADP for state 3 respiration measurements. Then, ATP synthesis was terminated by adding 3 μg oligomycin to achieve state 4 rate. This was followed by the addition of titrated concentration of FCCP protonophore (25–100 nM) to give uncoupled respiration or state 3. The complex III inhibitor anti-mycin (2 μM) was added to subtract non-mitochondrial respiration. Oxygen uptake is calculated in pmol min⁻¹ μg⁻¹ protein.

Complex I activity

Complex I activity was measured spectrophotometrically at 340 nm in mice liver mitochondria homogenate using the NADH method as described previously [17]. Liver mitochondria were obtained as for oxygen consumption measurement, except that the crude mitochondrial pellet was resuspended in KPi buffer and sonicated on ice 10 s 4 times to disrupt cell and mitochondrial membranes. Complex I activity was measured in an incubation volume of 1 ml containing 25 mM potassium phosphate buffer KPi pH 7.4 containing 4 mg ml⁻¹ BSA, 60 μM decylubiquinone, 80 μM NADH, 2 mM KCN and 2 μM antimycin at final concentrations. The reaction in each sample was started by the addition of mitochondrial protein (60 μg per sample) pre-treated with respective dye (DiOC₆(3), TD4-5, TD2-1 or TD2-2) for 5 min at 30 °C with constant shaking in dark. An intraindividual control preincubated without any dye was always examined in parallel. The rotenone insensitive complex I activity was determined simultaneously by measuring a sample with 4 μM rotenone added to the reaction. The decrease in absorbance was recorded for

4 min on a UV/vis spectrophotometer with an automatic water thermostated 12-cell holder in quartz cuvettes. The absorption coefficient of NADH used was 6.3 mM cm^{-1} , and the activities were expressed as $\mu\text{M NADH min}^{-1} \text{ mg}^{-1} \text{ protein}$.

Cellular oxygen consumption (Seahorse measurements)

Cellular oxygen consumption rates (OCR) were measured with XF96 Extracellular Flux Analyser and corresponding 'XF FluPak' (Seahorse Bioscience). U87-MG cells were seeded in Seahorse XF-96 plate at 20 000 cells per well. Prior to the assay cellular media was replaced with low-buffered DMEM media supplemented with TD21 (1 μM), TD22 (1 μM), DiOC₆(3) (100 nM) or no probe (control) and allowed to equilibrate for 1 h at 37 °C in a CO₂-free incubator. Before adding the probes, medium was enriched with 20 mM glucose, 1 mM pyruvate, and 2 mM glutamine and adjusted at pH 7.4. Basal OCR measurements were made followed by successive injection of oligomycin (1 $\mu\text{g ml}^{-1}$), carbonyl cyanide m-chlorophenyl hydra-zine CCCP (2 μM) and antimycin A (2.5 μM) to access proton leak, uncoupled and non-mitochondrial respiration, respectively.

Impedimetry for proliferation assay (xCELLigence) Cell attachment, spreading and proliferation were measured continuously under normal and treated conditions using the xCELLigence Real-Time Cell Analyzer (RTCA) system (ACEA Biosciences, Inc.). The cells were seeded in 16 well plate into 200 μl media at optimal density (15 000 cells/well) and monitored every 15 min for the next 120 h by measuring electrical impedance using the RTCA software.

Flow cytometry analysis of mitochondrial membrane potential

The cells ($1 \times 10^6 \text{ ml}^{-1}$) were incubated in 1 ml culture medium containing respective dyes for indicated amount of time in the dark at 30 °C (yeast) or 37 °C (human cell lines). Flow cytometry was carried out on a Becton-Dickinson FACSCalibur model equipped with a 488 nm argon laser and a 635 nm red diode laser. The collected data was analysed using BD CellQuest or FlowJo software version 7.2.5 for Micro-soft (TreeStar, San Carlos, CA, USA). The cells were gated and discriminated from background based on light scattering properties and PI exclusion.

Confocal microscopy

For confocal microscopy HeLa cells were seeded in culture medium and processed in 4-chamber glass bottom dish (Cellvis, Mountain View, CA) and analysed after staining procedure. The yeast cells were stained in suspension in 2 ml tubes as for the flow cytometry, protected from light with constant shaking at 450. After staining, the yeast cells were pelleted and

resulting pellets (5 μl) were mounted on microscope slides using low-melting-point agarose and imaged immediately.

To determine probe specificity for mitochondrial loading co-localisation of TD-dyes with Mitotracker Deep Red within mitochondria was used. Bleed-through was checked by imaging of samples labelled with a single fluorophore and acquiring dual channel images with the same setup used for the co-labelled system. The image and statistical analysis of colocalization and translocation kinetics was performed with ImageJ using JACoP plugin for calculating Pearson's correlation coefficients. Additionally, Van Steensel's method and Costes' randomisation test as previously described [18]. Images were also acquired in Z-stack mode with constant thickness of individual stack (depth interval = 4 μM , 10 Z-steps).

To assess the probe capacity to follow changes in $\Delta\psi\text{m}$ within individual cells, cultures were labelled with probes in the presence or absence of the complex III inhibitor antimycin or protonophor FCCP.

All images were acquired with a Leica TCS SP8 laser scanning confocal microscope, equipped with a 63 \times /1.3 NA oil immersion objective and a white light laser. Cells loaded with DiOC₆(3) were excited with the 484 nm laser line, and emission was detected in the 495–551 nm range. Cells loaded with Mitotracker Deep Red were excited with 644 nm laser line and emission was detected in the 661–700 nm range. Cells loaded with TD 4-5 were excited with the 470 nm laser line, and emission was detected in the 480–601 nm range. Cells loaded with TD 2-1 and TD 2-2 were excited with the 527 nm laser line, and emission was detected in the 540–570 nm range. Laser power and detector gain were identical for all experiments for a respective dye.

Statistical analysis

Statistical analyses of data were performed using R v2.15.3 (CRAN, <http://cran.r-project.org>) and RStudio for Windows, v0.97 (<http://rstudio.com/>). Before all analyses samples were tested for normality of distribution using the Shapiro–Wilk test, and one-way parametric ANOVA, followed by Dunnett's post hoc test for multiple comparisons of different groups against a control group. Where necessary, the Tukey's post hoc test for multiple comparisons was used. For all tests significance level was set at $p < 0.05$.

Results and discussion

Assessment of dye applicability for mitochondrial fluorescence readouts in yeast model in vivo

First, we evaluated the capacity of newly developed TD dyes to provide reliable mitochondria-specific fluorescence readouts. We performed a set of experiments of monitoring stained yeast cells by flow cytometry. After incubation in a wide range of dye concentrations

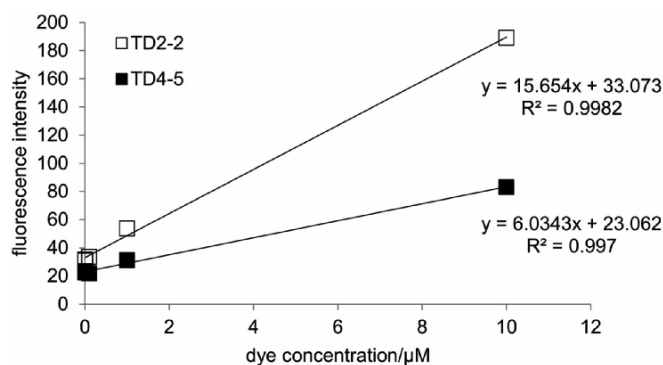


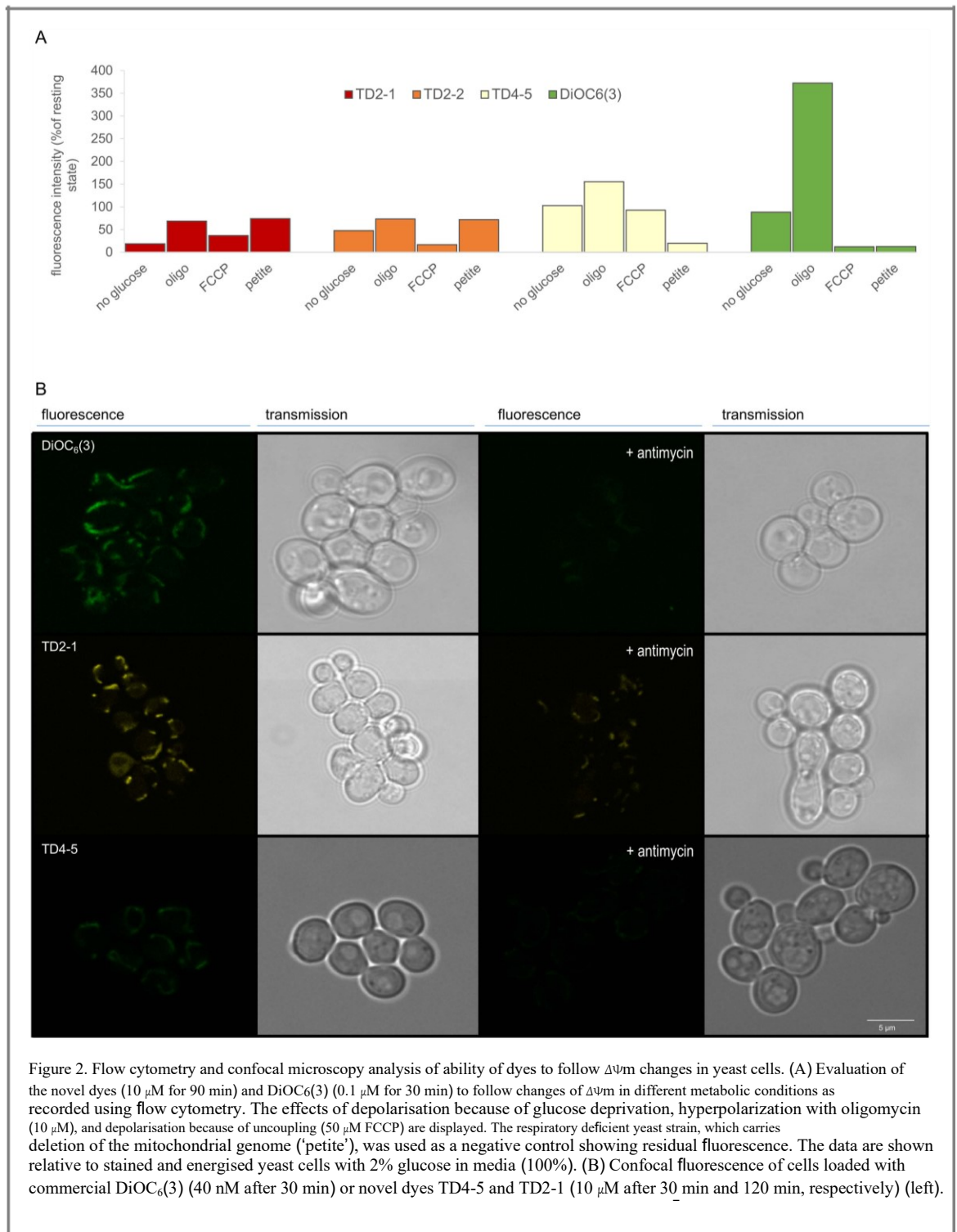
Figure 1. Flow cytometry analysis of the $\Delta\psi_m$ -related fluorescence of TD2-2 and TD4-5 in yeast cells to access the relationship of dye concentration and signal intensity. The yeast cells were incubated with TD dyes (0, 0.01, 0.1, 1 or 10 μM) and fluorescence intensity was monitored in FL-1 channel after 120 min or 60 min for TD2-2 and TD4-5, respectively. The results present the averaged fluorescent signal of technical duplicates of the sample.

(0.01–10 μM) or no dye, we found a linear relation between TD2-2 and TD4-5 dye concentration and fluorescence intensity, thus excluding significant interactions of dyes with other cellular targets (figure 1). In comparison to these dyes, TD2-1 dye showed much lower signal intensity (figure S1 is available at stacks.iop.org/MAF/5/015007/mmedia) although still with linear correlation between fluorescence and concentration (not shown). The experiments were also performed with the respiratory-deficient yeast cells, ('petite', characterised by the complete deletion of the mitochondrial genome). Both normal and 'petite' cells show weak baseline signal in the absence of dyes, which can be attributed to the light scattering in a cell (figure S1(a)). However, the addition of the dyes to cells resulted in a significant fluorescence increase proportional to the dye concentration. The difference in the fluorescence intensity between normal and 'petite' cells at 10 μM concentration and 1 h after staining was 3:1 (TD4-5) and 2:1 (TD2-2), respectively (not shown), as 'petite' mutants are expected to have smaller mitochondria, with a presumably lower $\Delta\psi_m$. However, TD-dyes showed relatively slow equilibration time between 60 and 120 min as determined with flow cytometry and confocal studies (figure S1) in comparison with DiOC₆(3), an established potential-dependent mitochondrial dye, where steady state fluorescence is reached within 15 min after staining [19].

Next, we evaluated the capacity of novel dyes to provide the reliable readouts in relation to changes in $\Delta\psi_m$ induced by pharmacological agents that affect $\Delta\psi_m$. In physiological conditions the maximal protonmotive force across the inner membrane is 180–220 mV. This range can be altered by the action of oligomycin (which slightly hyperpolarizes mitochondria by blocking proton re-entry via the ATP-synthase) or uncoupler such as FCCP which induces depolarisation. After loading of cells in different metabolic conditions (with or without glucose in medium, preincubation with oligomycin or FCCP) fluorescence

of cells was recorded using flow cytometry (figure 2(a)). The transition of dye-loaded yeast cells from resting state to de-energised state generated by glucose deprivation resulted in fluorescence decrease by 81% (TD2-1), 53% (TD2-2) and 12% (DiOC₆(3)), whereas TD4-5-loaded cells did not show significant fluorescence change. Pre-treatment of dye-loaded cells by oligomycin induced fluorescence signal increase for DiOC₆(3) and TD4-5 272% and 56% respectively, at variance to the fluorescence decrease in cells loaded by TD2-1 and TD2-2 by 32% and 27% respectively. The addition of FCCP decreased fluorescence intensity by 63%, 83%, 7% and 88% for TD2-1, TD2-2, TD4-5 and DiOC₆(3), respectively. 'Petite' yeast colonies (depleted mitochondria) were used as a negative control to measure residual fluorescence. However, absolute values in mV as well as the calibration of the fluorescent signal with tetraphenyl-phosphonium ion electrode are required to allow applications of here presented dyes as stand-alone standards.

Finally, we additionally evaluated the spatial dye specificity for mitochondrial compartmentalisation in yeast cells using confocal microscopy (figures S2 and 2(b)). As in flow cytometry experiments, DiOC₆(3) was used as positive control. All applied dyes showed bright fluorescence nicely localised within the yeast cell mitochondria (figure 2(b)). Moreover, treatment with antimycin resulted in complete loss of localised fluorescent response, both for TD-dyes as well as DiOC₆(3) (figure 2(b) left). As a specific inhibitor of respiratory chain complex III, antimycin blocks electron transport and thus mitochondrial potential accumulation [16, 20]. Therefore, the observed result of fluorescence decrease can be attributed to the antimycin-induced specific collapse of mitochondrial membrane potential, indicating that the accumulation of the TD-dyes was (a) mitochondrial and (b) directly dependent on $\Delta\psi_m$ since only mitochondria own respiratory complex III. Additionally, it is shown that there is no specific secondary target in cell for TD-dyes



and observed fluorescence in 'petite' cells (figure 2(b)) can be subtracted in flow cytometry experiments by ratiometric processing of fluorescence data.

Assessment of dye applicability in mammalian cell lines

As with yeast cells, flow cytometry was employed to determine optimal loading time and concentration for each probe in mammalian cells (figure 3). The major increase in fluorescent signal could be detected within 10 min with plateauing at first 30 min of loading.

Mammalian culture cells (HeLa) were also employed for confocal analysis to localise the fluorescent signal within the mitochondria, as determined by signal decrease because of FCCP treatment (figure 4(a)).

To specifically pinpoint the localisation of the probe signal within the subcellular compartments, colocalisation of the signal of the probes with the Mitotracker Deep Red was utilised. Mitotracker Deep Red specifically labels mitochondria compartment. Representative overlay picture is shown in figure 4(b). To quantify overlap between Mitotracker Deep Red

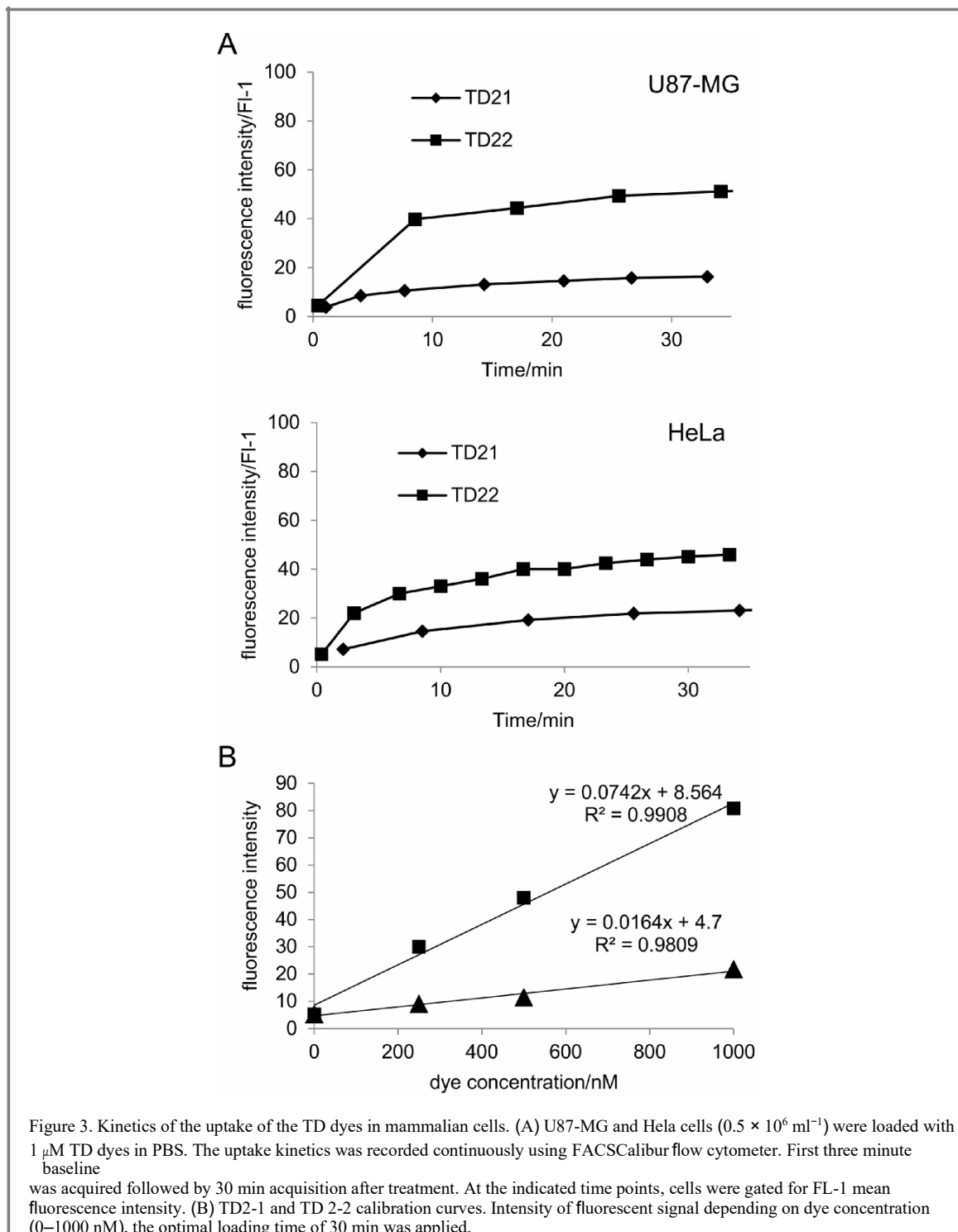


Figure 3. Kinetics of the uptake of the TD dyes in mammalian cells. (A) U87-MG and HeLa cells ($0.5 \times 10^6 \text{ ml}^{-1}$) were loaded with $1 \mu\text{M}$ TD dyes in PBS. The uptake kinetics was recorded continuously using FACSCalibur flow cytometer. First three minute baseline was acquired followed by 30 min acquisition after treatment. At the indicated time points, cells were gated for FL-1 mean fluorescence intensity. (B) TD-1 and TD-2 calibration curves. Intensity of fluorescent signal depending on dye concentration (0–1000 nM), the optimal loading time of 30 min was applied.

and TD probe signal Z-stacked images were used. Spatial correlation analysis showed good correlation between the signals with 0.63 ± 0.08 and 0.62 ± 0.06 Pearson's correlation coefficients (PCC) for TD21 and TD22, respectively. PCC can range from 1 to -1 , with 1 standing for complete positive correlation and -1 for a negative correlation, with zero standing for no correlation. Also, by using Van Steensel's method, dual channel images were shifted one in relation to another ($\pm 20 \text{ nm}$ maximum) and PCC obtained while operating a shift were plotted as a function of the displacement. Van Steensel's method showed a cross-correlation coefficient (CCF) values stacked in a

typical bell-shaped curve showing maximum PCC values with no shift of one Z-stacked image relative to other and minimum PCC values obtained after maximum displacement. Finally, Costes' randomisation test showed 100% degree of significance of higher original PCC values compared to randomised ones. Costes' statistical analysis is based on randomising green channel image by shuffling pixel blocks for 200 times for a single image and the PC is calculated each time between the random images of the green channel and the original image of the red channel. The PC for the original non-randomised images is then compared with the PCs of the randomised images and the

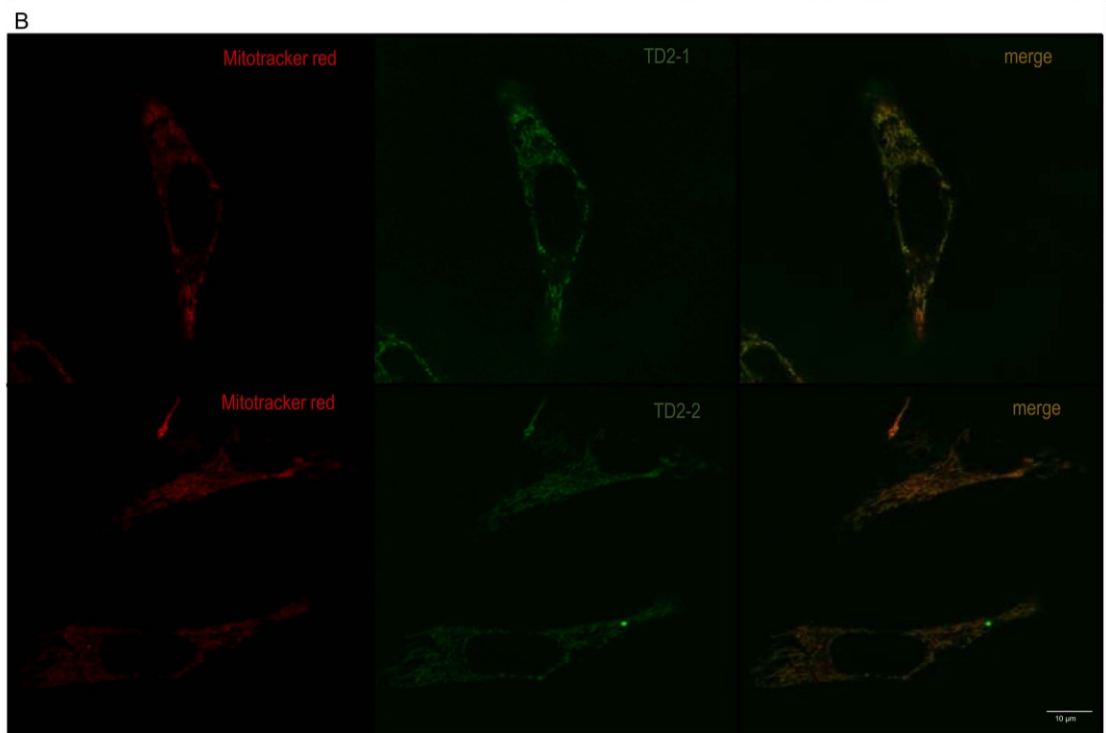
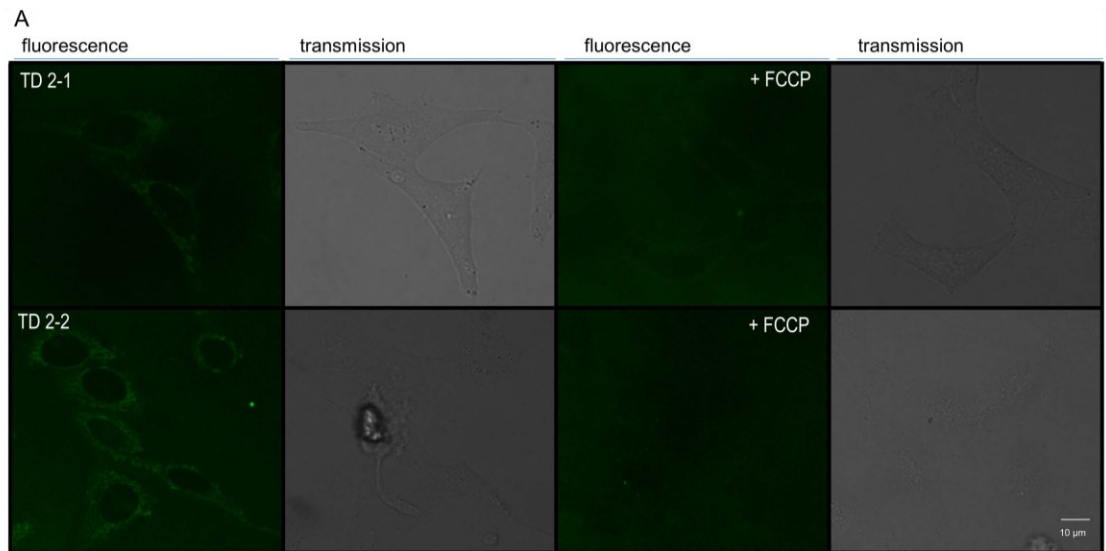


Figure 4. Confocal images of HeLa cells loaded with novel TD probes. (A) Fluorescence in cells loaded with 1 μM TD21 or TD22 for 30 min. Mitigated fluorimetric response in cells loaded with dyes in the presence of 2.5 μM FCCP. (B) Co-localisation of Mitotracker Deep Red and TD dyes in HeLa cells. The cells were loaded with Mitotracker Deep Red (20 nM for 15 min/37 $^{\circ}\text{C}$, red channel 661–700 nm) and either TD2-1 or TD2-2 (1 μM for 30 min/37 $^{\circ}\text{C}$, green channel 540–570 nm) and colocalisation of the signals (overlay) was assessed using ImageJ JACoP plugin. In representative image Pearson's correlation coefficients was showed to be 0.64 and 0.46 for TD2-1 and TD2-2, respectively. Van Steensel's method showed a cross-correlation coefficient (CCF) values stacked in a typical bell-shaped curve showing maximum PC values with no shift of one Z-stacked image relative to other and minimum PC values obtained after maximum displacement. Costes' randomisation test showed 100% degree of significance of higher original PC values compared to randomised ones.

significance (p -value) is calculated. The p -value, expressed as a percentage, is inversely correlated to the probability of obtaining the specified PC by chance (i.e. on randomised image pairs).

Assessment of dye toxicity on isolated mitochondria In order to be useful for the $\Delta\psi\text{m}$ measurement, the probe should be harmless to cell and without interference with the $\Delta\psi\text{m}$ itself. By using several approaches, we

accessed probe toxicity. First, we tested the probes directly on isolated mitochondria by evaluated the effect of the probes on mitochondria respiration. This process takes place within the mitochondrial inner membrane where electrons are transferred from NADH to oxygen through a chain of three large protein complexes complex I, III and IV. Electron flow within these transmembrane complexes leads to the transport of protons across the inner mitochondrial membrane

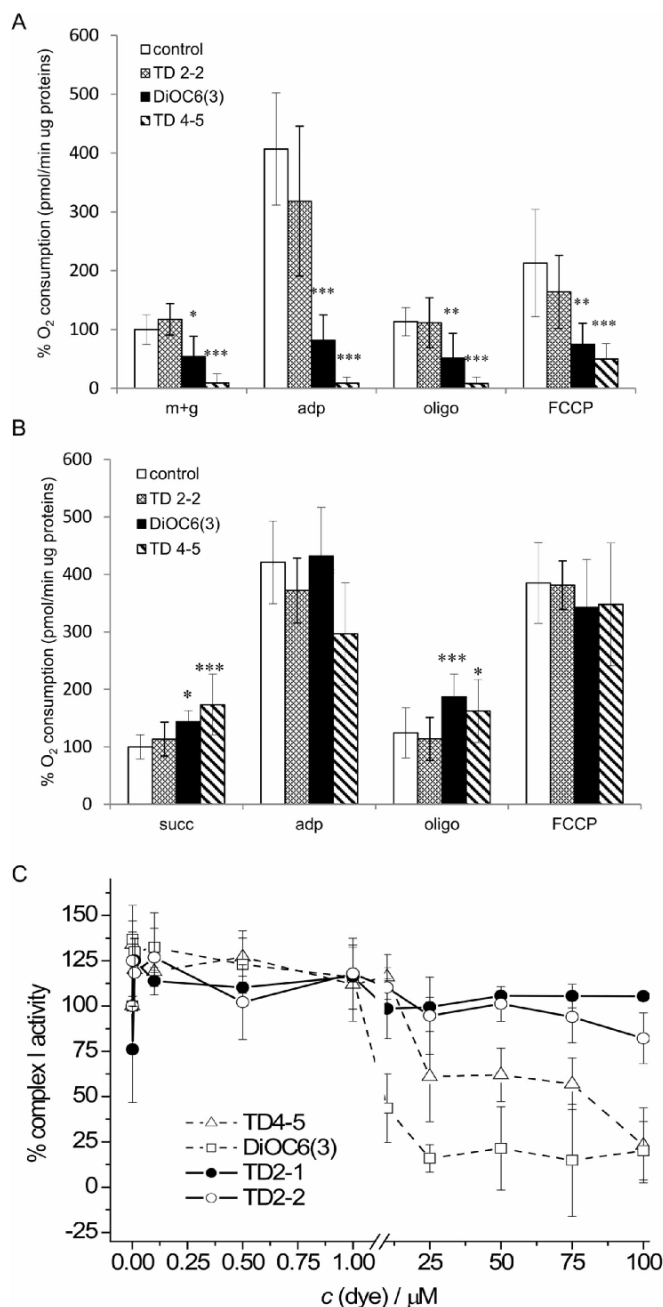


Figure 5. Evaluation of dye toxicity to mice liver mitochondria. Comparison of the effect of commercially available DiOC₆(3) versus novel dyes on mitochondrial respiration. Mice liver mitochondria were incubated using either glutamate/malate (A) or succinate/ rotenone (B) to feed complex I or complex II, respectively. All dyes were tested at 100 μM concentrations. After the incubation, mitochondrial suspension was analysed for oxygen consumption. For comparison, the data were normalised to 100% using the rate obtained in each preparation in the absence of dye. Each point represents the mean ± SD from at least 3 different mitochondria isolates each with 3 incubations. * p < 0.05 ** p < 0.01 *** p < 0.001. (C) Dose-dependent effect of dyes on enzymatic activity of complex I of the respiratory chain in mice liver mitochondrial homogenate. The data are shown as percentage of intraindividual control. Each point represents the average value from 2 to 3 measurements. Approximately 92 ± 6.7% of NADH conversion was complex I-dependent of (i.e., rotenone-sensitive).

creating $\Delta\psi_m$ necessary for ATP production. Complex II, in contrast with the other complexes, does not pump protons. It carries electrons from FADH₂, generated in succinate dehydrogenase in the citric acid cycle, to complex III. We demonstrated that a common $\Delta\psi_m$ indicator DiOC₆(3) (100 μM) markedly decreased mitochondrial respiration in the presence of respiratory complex I-feeding substrates (malate/glutamate, figure 5(a)), but not in the presence of respiratory

complex II-feeding substrate (succinate; figure 5(b)), suggesting the inhibition of complex I. Similar to DiOC₆(3), TD4-5 also inhibited respiration only in presence of complex I-feeding substrates. At variance to TD4-5 and DiOC₆(3), no inhibition on the respiration with any of the substrates used was observed with TD2-1 or TD2-2 (figures 5(a) and (b)).

To additionally confirm the hypothesis that DiOC₆(3) and TD4-5 interfere with complex I, we

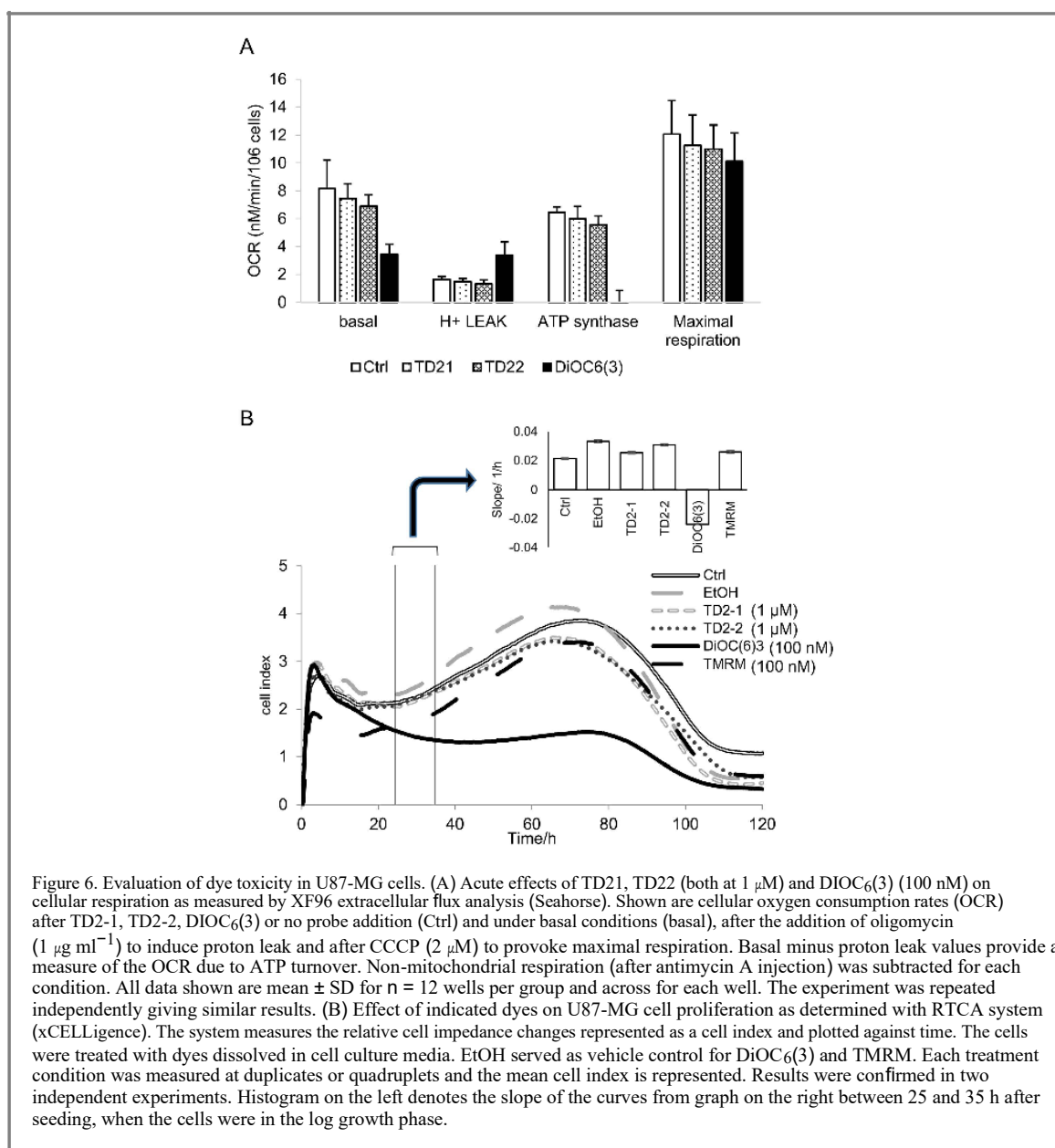


Figure 6. Evaluation of dye toxicity in U87-MG cells. (A) Acute effects of TD21, TD22 (both at 1 μM) and DiOC₆(3) (100 nM) on cellular respiration as measured by XF96 extracellular flux analysis (Seahorse). Shown are cellular oxygen consumption rates (OCR) after TD2-1, TD2-2, DiOC₆(3) or no probe addition (Ctrl) and under basal conditions (basal), after the addition of oligomycin (1 $\mu\text{g ml}^{-1}$) to induce proton leak and after CCCP (2 μM) to provoke maximal respiration. Basal minus proton leak values provide a measure of the OCR due to ATP turnover. Non-mitochondrial respiration (after antimycin A injection) was subtracted for each condition. All data shown are mean \pm SD for $n = 12$ wells per group and across for each well. The experiment was repeated independently giving similar results. (B) Effect of indicated dyes on U87-MG cell proliferation as determined with RTCA system (xCELLigence). The system measures the relative cell impedance changes represented as a cell index and plotted against time. The cells were treated with dyes dissolved in cell culture media. EtOH served as vehicle control for DiOC₆(3) and TMRM. Each treatment condition was measured at duplicates or quadruplets and the mean cell index is represented. Results were confirmed in two independent experiments. Histogram on the left denotes the slope of the curves from graph on the right between 25 and 35 h after seeding, when the cells were in the log growth phase.

made spectrophotometric analysis of the effect of dyes specifically on complex I activity in disrupted mitochondria. The concentration dependence study of liver mitochondria homogenate (figures 5(C) and S2) revealed that DiOC₆(3) and TD4-5 inhibited complex I activity already at 10 μM and 25 μM , respectively, while TD2-1 or TD2-2 did not have any inhibitory

effect even at extremely high concentration of 100 μM . Thus, by two mutually independent methods (oxygen electrode and spectrophotometric homogenate assay) it was shown that TD2-1 and TD2-2 do not suppress the complex I activity even at exceptionally high concentrations and prolonged times of incubation.

JC-1 is another commonly used cyanine dye.

Although the adverse effect on mitochondrial respiration was not revealed in this study (not shown), its non-coherent behaviour limits accurate measurement of $\Delta\Psi\text{m}$. The emission spectrum of JC-1 shifts from green to red with increasing concentration in the

mitochondria, thus allowing for a dual colour (green/red) and ratiometric semiquantitative assessment of large mitochondrial polarisation fluctuations [3]. Therefore, typical JC-1 usage relies on threshold effects, which precludes its usage for reliable detection of subtle gradations in $\Delta\Psi\text{m}$. Additionally, aggregate (i.e., red) JC-1 fluorescence may change independently of $\Delta\Psi\text{m}$, while green fluorescence is not limited to the mitochondrial membranes [21].

Toxicity testing in mammalian cell lines

Additional tests were performed to assess TD2-dye series toxicity on intact mammalian cell lines and in real-time. To study the influence of the probes on cellular bioenergetics, extracellular flux (XF) analyser was employed where OCR is used to measure mitochondrial respiration in cellular milieu. U87-MG cell line was treated with TD21 and TD22 (both at 1 μM) for 1 h, and then respiration was determined in basal

conditions, under inhibition of ATP synthesis after oligomycin addition, then after adding the uncoupler CCCP to determine the maximal respiratory capacity, and finally by addition of antimycin A to determine non-mitochondrial respiration (figure 6(a)). The results show that probes are innocuous to cellular bioenergetics, while DiOC₆(3) showed toxic effect inhibiting ATP synthase activity as well as inhibiting the uncoupled respiration. Contrary to DiOC₆(3), TD probes proved to be innocuous, showing no effect on any of respiration modules employed (figure 6(a)).

Next we used marker-free and real-time cell monitoring xCELLigence system to access long term effect of the dyes on cell proliferation. In U87-MG (figure 6(b)) and HeLa (figure S3) cell lines TD2-1 and TD2-2 showed no effect on cell proliferation. In contrast, DiOC₆(3) completely inhibited cell proliferation and reduced cell index values to zero as determined by measuring cell impedance during the 120 h period. TMRM was employed as negative standard given it is the least toxic to currently used probes. As expected, TMRM showed no toxic effect on cell proliferation at 100 nM concentration used.

Collectively, these results confirmed that newly synthesised probes TD 2-1 and TD 2-2 are completely non-toxic contrary to DiOC₆(3) and TD4-5 which inhibit cellular respiration.

Conclusions

To be reliable tools for assessment of mitochondria functionality, fluorescent probes need to have specific and strong signal related to mitochondrial potential. On top of that, probe need to be nontoxic and without perturbations of the effects they are supposed to measure.

Confocal microscopy and flow cytometry used in conjunction with fluorescent $\Delta\Psi_m$ -dependent probes, are the most suitable methods for the investigation of the mitochondrial function in live cells. Flow cytometry is specifically suitable for a large number of cells, notably heterogeneous cell populations. DiOC₆(3) is one of the most commonly used probes for this purpose but its high toxicity toward mitochondrial respiration, and its ultra-low (<1 nM) concentrations necessary to accurately measure $\Delta\Psi_m$, limit the utility of this probe, especially in quenching mode where higher concentrations are required [8, 10]. In our hands, DiOC₆(3) inhibited respiration of isolated mitochondria with complex I substrates employed as well as directly inhibiting complex I activity in disrupted liver mitochondria. Moreover, exposure to DiOC₆(3) resulted in decreases in key bioenergetic cell parameters (figure 6(a)) resulting with drastically inhibited cell proliferation on the long term (figure 6(b)). As opposed to DiOC₆(3), the novel phosphonium derivatives TD2-1 and TD2-2 probes proved to be remarkably innocuous and completely

nontoxic to mitochondrial (figures 5(a) and (b)) or cell respiration (figure 6(a)) and no interference with complex I activity was seen even at high 100 μ M concentrations (figure 5(c)). Even after long term incubation and five days of assessment, novel probes showed to be completely inert in terms of cell division cycle (figure 6(b)). Confocal microscopy and flow cytometry experiments confirmed applicability of novel dyes for monitoring the $\Delta\Psi_m$ in cells. Specific labelling of the mitochondrial compartment was shown using confocal microscopy by localising the fluorescent signal of the probes with Mitotracker Deep Red (figure 4(b)) and also by mitigating the probe signal with protonophore as well as respiratory complex inhibition (figures 4(a) and 2(b)).

Therefore, probes showed to respond to mitochondria-potential changes as evidenced by the flow cytometry analysis (figures 1 and 2(a)), as well as microscopy studies (figures 2(b) and 4). Dissipation of mitochondria potential using complex III inhibitor antimycin and CCCP uncoupler ceased mitochondria-related fluorescent signal of TD-dyes. Although DiOC₆(3) seems to have a much stronger fluorescent signal that follows mitochondria potential fluctuations in more sensitive fashion (figure 2(a)), the TD 2-1 and TD2-2 probes still characterize as $\Delta\Psi_m$ -sensitive and require live and functional mitochondria for staining. Larger conjugation structures are proposed to improve the brightness of small fluorescent probes [22]. On the other hand, TD4-5 dye showed inhibitory effect on mitochondrial respiration comparable to the effect of DiOC₆(3) (figure 5). Enzymatic assay confirmed that TD4-5 inhibits complex I activity although to a lesser extent than DiOC₆(3), given that higher concentration (25 versus 10 μ M) was necessary for inhibitory effect to be evident.

Contrary to the TD2 series, TD4-5 dye showed an inhibitory effect on mitochondrial respiration comparable to the effect of DiOC₆(3) (figure 5). Enzymatic assay confirmed that TD4-5 inhibits complex I activity although to a lesser extent than DiOC₆(3), given that higher concentration (25 versus 10 μ M) was necessary for the inhibitory effect to be evident. TMRM remains one of the most preferred probes because of its least toxicity in conjunction with fine detection of gradations of differences in $\Delta\Psi_m$ [8]. However TMRM can be used in concentrations only up to 0.5 μ M without causing an inhibitory effect on respiration [12]. TMRM is a red-orange dye with emission maximum at $\lambda = 580$ nm. Having a dye that complements TMRM in spectral range without toxic side effects would be of benefit. TD2-1 and TD2-2 at $\lambda = 547$ nm (green) emission peak fulfil this purpose, and that is one of the most important features that these new dyes provide.

In conclusion, TD2-1 and TD2-2 probes showed specific and potential dependent mitochondria-related fluorescent signal, without exhibiting any toxic effect to cell functioning. The comparison of the novel

Table 2. Comparison of newly reported and mostly used fluorescent potential-dependent probes for mitochondria.

Probe used	Equilibration time	Preferred usage	Toxicity	Solubility
TD2-1	30 min	Confocal microscopy	Non toxic to cell respiration or proliferation even at 1 μ M concentration (this study)	Water ^{13,14}
TD2-2	30 min	Confocal microscopy	Non toxic to cell respiration or proliferation even at 1 μ M concentration (this study)	Water ^{13,14}
TD4-5	120 min	N/A	Inhibits mitochondrial respiration and complex I activity starting from extremely high concentration of 25 μ M (this study)	Ethanol, DMSO ^{13, 14}
TMRM	60 min ¹⁰	Flow cytometry and confocal microscopy ^{8,10}	Up to 0.5 μ M without causing an inhibitory effect on respiration [20]	Ethanol, DMSO
DiOC ₆ (3)	15 min ¹⁰	A measure of $\Delta\psi_m$ by flow cytometry studies	Significant inhibition of respiration above 2 nM [10] inhibits cell respiration and proliferation at 100 nM (this study)	Ethanol, DMSO

probes with the mostly used DiOC₆(3) and TMRM is summarized in table 2. The biggest drawback, detected so far, seems to be relatively lower fluorescent intensity compared to DiOC₆(3) as detected by flow cytometry (figure 2(a)).

Another attractive property of novel TD-dyes is their high solubility ($c > 10$ mM) and exceptional chemical stability in aqueous solutions [13, 14], giving them advantage over other commercial dyes which mostly require toxic DMSO or ethanol as solvent for stock solutions.

Acknowledgments

This project has been funded by EU Marie Curie FP7-PEOPLE-2011-COFUND program, NEWELPRO, European Commission Grant Agreement No.291823; Ministry of Science, Education, Sport of Croatia Grant Numbers 098-0982464-13 and 098-0982914-2918; and InnoMol FP7-REGPOT-2012-2013-1 Grant Agreement Number 316289. Anita Kriško from Med-ILS is acknowledged for kindly providing us all *S. cerevisiae* cultures. Lucija Horvat is acknowledged for help in confocal microscopy.

References

- [1] Tuppen H A L, Blakely E L, Turnbull D M and Taylor R W 2010 *Biochim. Biophys. Acta* **1797** 113

- [2] Zamzami N, Marchetti P, Castedo M, Zanin C, Vayssières J L, Petit P X and Kroemer G 1995 *J. Exp. Med.* **181** 1661
- [3] Nicholls D G 2004 *Aging Cell* **3** 35
- [4] Dickinson B C and Chang C J 2008 *J. Am. Chem. Soc.* **130** 9638
- [5] Wang X H, Peng H S, Yang L, You F T, Teng F, Hou L L and Wolfbeis O S 2014 *Angew. Chemie* **53** 12471
- [6] Wang X H, Peng H S, Yang W, Ren Z D and Liu Y A 2016 *Microchimica Acta* **183** 2723
- [7] Cottet-Rousselle C, Ronot X, Leverve X and Mayol J F 2011 *Cytometry A* **79** 405
- [8] Perry S W, Norman J P, Barbieri J, Brown E B and Gelbard H A 2011 *Biotechniques* **50** 98
- [9] Nicholls D G and Ward M W 2000 *Trends Neurosci.* **23** 166
- [10] Rottenberg H and Wu S 1998 *Biochim. Biophys. Acta* **1404** 393
- [11] Modica-Napolitano J S and Aprile J R 1987 *Cancer Res.* **47** 4361
- [12] Scaduto R C Jr and Grotyohann L W 1999 *Biophys. J.* **76** 469
- [13] Tumir L M, Crnolatac I, Deligeorgiev T, Vasilev A, Kaloyanova S, Grabar Branilović M, Tomić S and Piantanida I 2012 *Chem. Eur. J.* **18** 3859
- [14] Crnolatac L M, Tumir N Y, Lesev A A, Vasilev T G, Deligeorgiev K, Miskovic L, Glavas-Obrovac O, Vugrek and Piantanida I 2013 *Chem. Med. Chem.* **8** 1093
- [15] Ross M F, Kelso G F, Blaikie F H, James A M, Cochemé H M, Filipovska A, Da Ros T, Hurd T R, Smith R A and Murphy M P 2005 *Biochemistry* **70** 222
- [16] Silva M and Oliveira P J 2012 *Methods Mol. Biol.* **810** 7
- [17] Long J, Ma J, Luo C, Mo X, Sun L, Zang W and Liu J 2009 *Life Sci.* **85** 276
- [18] Bolte S and Cordelières F P 2006 *J. Microsc.* **224** 213
- [19] Petit P X, Glab N, Marie D, Kieffer H and Metzseau P 1996 *Cytometry* **23** 28
- [20] Brand M D and Nicholls D G 2011 *Biochem. J.* **435** 297
- [21] Bernardi P, Scorrano L L, Colonna R, Petronilli V and Di Lisa F 1999 *Eur. J. Biochem.* **264** 687
- [22] Shi W, Li X and Ma H 2014 *Methods Appl. Fluoresc.* **2** 042001